

AD-A075 897

NAVAL RESEARCH LAB WASHINGTON DC  
FRACTOGRAPHIC AND MICROSTRUCTURAL ANALYSIS OF FATIGUE SPECIMENS--ETC(U)  
SEP 79 G GABETTA , V PROVENZANO

F/G 11/6

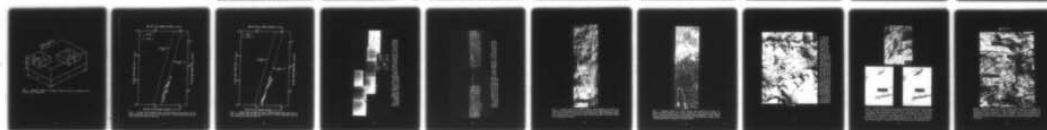
UNCLASSIFIED

NRL-MR-4062

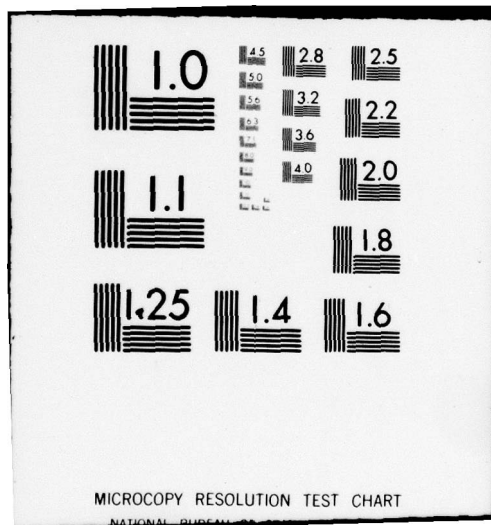
NUREG-CR-0968

NL

| OF |  
AD  
A075897



END  
DATE  
FILMED  
11 -79  
DDC



MICROCOPY RESOLUTION TEST CHART  
NATIONAL BUREAU OF STANDARDS-1963-A

**LEVEL II**

✓ **NRL Memorandum Report 4062**  
✓ **NUREG/CR-0968**

12 b.s.

AD A075897

**Fractographic and Microstructural Analysis of  
Fatigue Specimens of A302 Grade B Steel  
Tested in Air at Room Temperature**

**G. GABETTA AND V. PROVENZANO**

*Thermostructural Materials Branch  
Material Science and Technology Division*

September 28, 1979

Prepared for U.S. Nuclear Regulatory Commission



DDC  
RECEIVED  
OCT 31 1979  
RECEIVED  
D

**NAVAL RESEARCH LABORATORY**  
Washington, D.C.

Approved for public release; distribution unlimited.

79 10 01 031

### NOTICE

This report was prepared as an account of work sponsored by an agency of the United States Government. Neither the United States Government nor any agency thereof, or any of their employees, makes any warranty, expressed or implied, or assumes any legal liability or responsibility for any third party's use, or the results of such use, of any information, apparatus, product or process disclosed in this report, or represents that its use by such third party would not infringe privately owned rights.

The views expressed in this report are not necessarily those of the U. S. Nuclear Regulatory Commission.

Available from  
U. S. Nuclear Regulatory Commission  
Washington, D.C. 20555

UNCLASSIFIED

18 NUREG  
19 CR-0968

SECURITY CLASSIFICATION OF THIS PAGE (When Data Entered)

REPORT DOCUMENTATION PAGE		READ INSTRUCTIONS BEFORE COMPLETING FORM
1. REPORT NUMBER NRL Memorandum Report 1062 NUREG/CR-0968	2. GOVT ACCESSION NO.	3. REPORT'S CATALOG NUMBER 9
4. TITLE (and Subtitle) FRACTOGRAPHIC AND MICROSTRUCTURAL ANALYSIS OF FATIGUE SPECIMENS OF A302 GRADE B STEEL TESTED IN AIR AT ROOM TEMPERATURE	5. DATE OF REPORT & PERIOD COVERED Progress report, a continuing NRL problem	6. PERFORMING ORG. REPORT NUMBER
7. AUTHOR(s) G. Gabetta* V. Provenzano	8. CONTRACT OR GRANT NUMBER(s) NRC FIN B5528 Interagency Agr. RES-79-103	
9. PERFORMING ORGANIZATION NAME AND ADDRESS Naval Research Laboratory Washington, DC 20375	10. PROGRAM ELEMENT, PROJECT, TASK AREA & WORK UNIT NUMBERS NRL Problem MO1-40	
11. CONTROLLING OFFICE NAME AND ADDRESS U.S. Nuclear Regulatory Commission Office of Nuclear Regulatory Research Washington, DC 20555	11.28 12.22	12. REPORT DATE Sep 1979 13. NUMBER OF PAGES 20
14. MONITORING AGENCY NAME & ADDRESS (if different from Controlling Office)	15. SECURITY CLASS. (of this report) UNCLASSIFIED	15a. DECLASSIFICATION/DOWNGRADING SCHEDULE
16. DISTRIBUTION STATEMENT (of this Report) Approved for public release; distribution unlimited.		
17. DISTRIBUTION STATEMENT (of the abstract entered in Block 20, if different from Report)		
18. SUPPLEMENTARY NOTES *Current address: Centro Informazioni Studi Esperienze (CISE), Research Laboratory, Milan, Italy Prepared for the U.S. Nuclear Regulatory Commission under Agreement RES-79-103 and as part of a cooperative program with the Italian Electric Power Company (ENEL). NRC Distribution Category R5		
19. KEY WORDS (Continue on reverse side if necessary and identify by block number) Energy dispersive X-ray analysis Fatigue crack propagation Fractography Inclusion bands Metallography Nuclear pressure vessel steel Preferential decohesion		
20. ABSTRACT (Continue on reverse side if necessary and identify by block number) Microscopic studies were undertaken to characterize the failure processes and to establish correlations with fatigue crack propagation data of Type A302-B ferritic steel tested in air at room temperature. A cooperative program was established between the Naval Research Laboratory (NRL) and the Centro Informazioni Studi Esperienze (CISE) to investigate the fatigue properties of this ferritic steel for nuclear pressure vessel applications. Failed specimens have been examined by scanning electron microscopy (SEM), by metallographic techniques, and by energy dispersive x-ray (Continues)		

DD FORM 1 JAN 73 1473

EDITION OF 1 NOV 65 IS OBSOLETE  
S/N 0102-014-6601

UNCLASSIFIED

SECURITY CLASSIFICATION OF THIS PAGE (When Data Entered)

251950

4/B

20. Abstract (Continued)

microanalysis. SEM examination of the fracture surfaces of specimens cut in the T-L direction revealed the presence of inclusion bands above an observed  $\Delta K$  threshold value. Subsequent x-ray image scans and corresponding energy spectra showed that the bands were manganese-sulfide inclusions. The inclusion bands resulted in increased crack growth rate in these specimens compared to those cut in the L-T orientation specimens. The  $\Delta K$  threshold value necessary to activate the inclusion bands is thought to be a measure of the cohesive strength between the inclusions and the material matrix. The failure mode of all the specimens tested was transgranular; extensive microcracking was also present in the fracture surfaces. The microcracking did not appear to have affected the crack propagation behavior.

Accession For	
NTIS GMAI	<input checked="" type="checkbox"/>
DDC TAB	<input type="checkbox"/>
Unannounced	<input type="checkbox"/>
Justification	
By	
Distribution/	
Availability Codes	
Dist	Avail and/or special
A	

DDC  
RECEIVED  
OCT 31 1979  
D

## CONTENTS

INTRODUCTION	1
EXPERIMENTAL PROCEDURE	2
RESULTS AND DISCUSSION	2
SUMMARY AND CONCLUSIONS	5
ACKNOWLEDGMENTS	6
REFERENCES	7

# FRACTOGRAPHIC AND MICROSTRUCTURAL ANALYSIS OF FATIGUE SPECIMENS OF A302 GRADE B STEEL TESTED IN AIR AT ROOM TEMPERATURE

## INTRODUCTION

The studies of fatigue crack propagation (FCP) behavior in ferritic steels for pressure vessel applications are of primary importance to light water reactor safety. One of many objectives of current FCP studies is to test the validity of ASME Code Section XI curve for materials in nuclear environments. In addition, these studies are aimed at understanding the complex mechanisms of fatigue failure as a function of the significant variables which include material condition and environment.

The light water reactor safety programs involving the ferritic steels are of interest to many countries. In Italy, a research program in this field is sponsored by The Italian Electric Power Company (ENEL) and is being carried out at the Centro Informazioni Studi Esperienze (CISE) Research Laboratory in Milan, Italy. At the CISE laboratory an autoclave system for conducting fatigue tests at elevated temperatures in pressurized water environment will soon be operational. In support of the planned CISE research program for ENEL, preliminary FCP tests in air at room temperature were performed on low-shelf A302-B steel procured by the Naval Research Laboratory (NRL) to characterize early production nuclear pressure vessels. In connection with fatigue and fracture studies on the ferritic steels for pressure vessel applications, a cooperative research program has been established between NRL and CISE. The results reported are part of this cooperative program which is sanctioned and encouraged by the U. S. Nuclear Regulatory Commission (NRC).

Since the rolling procedure used in steel making is known to affect the microstructure of A302-B steel [1], preliminary tests were designed to investigate the effect of rolling direction on the FCP behavior of this ferritic steel. The FCP tests included in the present study were conducted at the CISE laboratory; the fractographic, metallographic and X-ray microanalysis studies on the failed specimens have been carried out at NRL.

In the present study, the fractographic and microstructural observations are correlated to the corresponding mechanical data in order to characterize the failure processes and to gain additional insight into the mechanisms of fatigue failure of this ferritic steel.

Note: Manuscript submitted July 11, 1979.

## EXPERIMENTAL PROCEDURE

The chemical composition of the A302-B steel plate is given in Table 1. Two sets of 1/2-in. compact tension specimens were tested. Each set consisted of two specimens, one cut in T-L and the other in the L-T orientation (Fig. 1).<sup>\*</sup> All fatigue tests were conducted in air at room temperature using a constant specimen deformation procedure; the applied load was sinusoidal with a frequency of 13.3 Hz. In this procedure, the value of  $\Delta K$  increases with crack length, even though the applied load is gradually decreased as the length increases. Additional details concerning the testing procedure are reported elsewhere [2].

In order to minimize any possible effect of a crack initiation phenomenon, the specimens were precracked to a length of 1.25 mm using the same waveform and frequency as employed for the tests themselves. One set of specimens was machined to a relative crack depth,  $a/W$ , of 0.44 and the other to an  $a/W$  of 0.30. Starting  $\Delta K$  values for the two sets of specimens were 22 MPa $\sqrt{m}$  (20 ksi  $\sqrt{in.}$ ) and 16.5 MPa $\sqrt{m}$  (15 ksi  $\sqrt{in.}$ ), respectively. During cycling, the crack length was monitored by means of a travelling microscope. When the crack length,  $a$ , had increased by about .25 mm (0.01 in.), the test was temporarily stopped and the values of maximum load, minimum load, and crack length were recorded. The values of  $\Delta K$  were then computed according to the formula listed in ASTM E-399 [3]. For each test, the log  $da/dN$  vs log  $\Delta K$  curve was obtained by using a 7 point incremental polynomial technique, as recommended by ASTM E647-78T [4].

After completion of the tests, the first set of specimens were fractured at liquid nitrogen temperature. The fracture surfaces were then examined with a scanning electron microscope (SEM), using an ISI Super II SEM operated in the high voltage mode. The second set of specimens were used for metallographic examination. Transverse sections were cut perpendicular to the fracture surface along the specimen midplane and polished. The sections were etched with a solution consisting of 1 percent nital and 2 parts of 4 percent picral solution. The polished and etched sections were examined both optically and with the SEM. The optical micrographs were taken using a Bausch and Lomb Research II metallograph. Once the examination on the polished sections was completed, the sections were broken apart at liquid nitrogen temperature and their fracture surfaces were examined with the SEM.

## RESULTS AND DISCUSSION

The FCP data obtained from the specimen tests are presented in Figs. 2 and 3. As shown by both figures, all of the crack growth data fell close to the ASME Section XI air line. The crack growth rates for the first set of specimens (Specimen VADA1, cut in the T-L direction, and Specimen VADA2, cut in the L-T direction) ran roughly parallel to each other for most of the  $\Delta K$  range, with the T-L specimen (VADA1) exhibiting the higher crack growth rate (Fig. 2). The crack growth rates for the second set of specimens (VAB1, cut in the T-L direction, and VAB2, cut in the L-T direction) were about equal for  $\Delta K$  values below 33 MPa $\sqrt{m}$  (30 ksi  $\sqrt{in.}$ ). Above this  $\Delta K$  value, the crack growth rate of the T-L specimen

<sup>\*</sup>The identification convention used is that suggested by ASTM E-399 (3) and is illustrated in Fig. 1.

TABLE 1

## Chemical Composition of A302-B Steel

<u>Elements</u>	<u>Content (wt-%)</u>
C	0.210
Mn	1.460
P	0.010
S	0.021
Si	0.240
Ni	0.230
Cr	0.060
Mo	0.540
V	0.012
Cu	0.059
As	0.004
Sn	0.009
Al	0.034
Ti	0.008
Co	0.012
Ta	0.020
B	0.001
Pb	0.004
Cb	0.007
Fe	Bal.

(VAB1) was higher (Fig. 3). The difference in the crack growth behavior in the two sets of specimens was not large. It is interesting to point out however, that a lower starting  $\Delta K$  resulted in a higher growth rate (the starting  $\Delta K$  for VAB1 and VAB2 was  $16.5 \text{ MPa}\sqrt{\text{m}}$  while for VADA1 and VADA2 it was  $22 \text{ MPa}\sqrt{\text{m}}$ ). Since the basic objective of the mechanical tests was to investigate the effect of specimen orientation on the fatigue behavior the effect of starting  $\Delta K$  on FCP will not be critically evaluated in this report.

The relationships between the crack path and the microstructure are illustrated by the photomicrographs shown in Figs. 4 and 5. The photomicrographs in Fig. 4 refer to specimen VAB1 (T-L) while the micrographs presented in Fig. 5 refer to specimen VAB2 (L-T). The two crack profiles show that extensive crack branching is present in both specimens. The degree of crack branching, as indicated by the secondary cracks, becomes more pronounced in the high  $\Delta K$  region. In the region of high  $\Delta K$ , where the crack propagation rate is higher, the microcracks associated with crack branching are smaller in size and required a higher magnification to reveal their presence. The reduction in the average size of the microcracks in the high  $\Delta K$  regime did not appear to have affected the crack propagation behavior. Crack branching usually has the effect of slowing the crack propagation rate by distributing the stresses at the crack tip; this did not seem to have been the case in these two specimens.

The significant fractographic features observed in the SEM examinations of fracture surfaces are summarized by the micrographs presented in Figs. 6-8. In the T-L specimen (VADA1), a microstructural texture running parallel to the macroscopic crack propagation direction is present (Fig. 6). In the second set of tests the T-L specimen (VAB1) shows an increase in the crack growth rate at  $\Delta K$  values of  $25\text{--}30 \text{ MPa}\sqrt{\text{m}}$  (Fig. 3) that coincides with the appearance of the parallel texture in the fracture surface (Fig. 7). In the L-T specimen (VAB2), whose corresponding crack growth rate was lower, the parallel texture was absent. The failure mode for T-L specimen was transgranular with secondary cracking perpendicular to the macroscopic crack propagation direction (Fig. 8). Similar fractographic features have been observed in other ferritic steels tested under analogous experimental conditions [5,6].

As observed above, the fracture surface of T-L specimen (VAB1) is characterized by a parallel texture when  $\Delta K$  exceeds a minimum value in the range of  $25\text{--}30 \text{ MPa}\sqrt{\text{m}}$ . This texture is thought to arise from inclusion bands that are present in the rolled material. These inclusions became elongated during the rolling procedure. To see if the parallel texture is indeed the result of the inclusion bands, the fracture surface was analyzed with an X-ray microanalyzer that is attached to an AMR 1000 scanning electron microscope. The results of the X-ray microanalysis are summarized in Fig. 9. The analysis confirms that the parallel features were manganese-sulfide inclusion bands.

It appears, therefore, that inclusion bands are the primary cause for the increase in the crack growth rate above a minimum  $\Delta K$  value. It is believed that a preferential decohesion process occurs at the inclusion-matrix interface, which become activated above some threshold stress level and resulted in higher crack growth rates. This threshold stress is probably a measure of the bond strength between the inclusion and the material matrix. The inclusion effect is directional,

due to the strong directionality of the inclusion band that is related to the rolling process (1). Therefore, the T-L specimens showed a higher crack growth rate when compared to the L-T case.

The SEM micrograph shown in Fig. 10 typifies the fractographic features observed in the L-T specimens (VADA2 and VAB2). As illustrated by the micrograph, only a small inclusion band was present though some lamina-shaped holes were seen. These holes are believed to represent the inclusion bands that are oriented perpendicular to the crack plane. Since most of the inclusion bands in the L-T specimens are preferentially oriented perpendicular to the main crack path, the few bands that resided along the crack plane did not seem to have had an affect on crack propagation behavior.

#### SUMMARY AND CONCLUSIONS

The fracture surfaces and the microstructure of A302-B ferritic steel FCP specimens tested at room temperature have been examined by scanning electron microscopy (SEM), by metallographic techniques, and by energy dispersive X-ray microanalysis. The crack propagation was taken in the T-L and L-T test directions to permit an investigation of the effect of rolling direction on the fatigue crack growth. The results may be summarized as follows:

- (1) Inclusion bands in the T-L specimens were strongly aligned in the rolling direction and were observed in the fracture surfaces. The composition of inclusion bands was determined by energy dispersive X-ray microanalysis; the X-ray microanalysis showed them to be manganese-sulfide inclusions. These bands indicate a preferential decohesion process at the matrix-inclusion interface that resulted in higher crack growth rates in the T-L specimens when compared to the crack growth rates of the L-T specimens.
- (2) In the T-L specimen which had been tested with a lower starting  $\Delta K$  value, inclusion bands were not observed unless  $\Delta K$  exceeded a minimum value in the range of 25-30 MPa $\sqrt{m}$  (22.7-27.3 ksi $\sqrt{in.}$ ). The minimum  $\Delta K$  value is probably related to the bond strength between the inclusions and the material matrix
- (3) A few small inclusion bands were seen in the fracture surfaces of the L-T specimens. These small inclusions did not appear to have affected the fatigue crack growth behavior of the material cut in L-T direction. However, some lamina-shaped holes were present and are thought to represent the inclusion bands oriented perpendicular to the crack plane. The presence of few inclusions and the lamina-shaped holes showed, as anticipated, that the inclusion bands in the L-T specimens were mostly oriented perpendicular to the main crack path.
- (4) Consistent with similar fatigue studies in other ferritic steels, the failure mode in all the specimens tested was transgranular with extensive secondary cracking. The secondary cracking did not appear to affect the fatigue properties.

## ACKNOWLEDGMENTS

This study was sponsored by the U. S. Nuclear Regulatory Commission (NRC), Division of Reactor Safety Research, Metallurgy and Materials Branch, and by the Italian Electric Power Company (ENEL). Also, the authors wish to express their appreciation to Drs. F. J. Loss and F. A. Smidt, Jr., and to J. R. Hawthorne for the many constructive comments.

## REFERENCES

1. F. A. Heiser and R. W. Hertzberg, "Anisotropy of Fatigue Crack Propagation," Trans. ASME, J. Basic Engineering, June 1972, Series D, Vol. 93, pp. 211-217.
2. G. Gabetta, CISE Technical Note (to be published).
3. "Standard Method of Test for Plain-Strain Fracture Toughness of Metallic Materials," ASTM Designation E399-70T, ASTM Standards, Part 10, pp. 512-533, 1978.
4. "Tentative Method of Test for Constant Load-Amplitude Fatigue Crack Growth Rate Above  $10^{-8}$  m/cycle," ASTM Designation E647-78T, ASTM Standards, Part 10, pp. 662-682, 1979.
5. C. E. Richards and T. C. Lindley, Engineering Fracture Mechanics, Vol.4, pp. 951-958, 1972.
6. W. C. Cullen, et. al. "Fatigue Crack Growth of A508 in High-Temperature, Pressurized Reactor-Grade Water," NRL Memorandum Report, Naval Research Laboratory (pending publication).

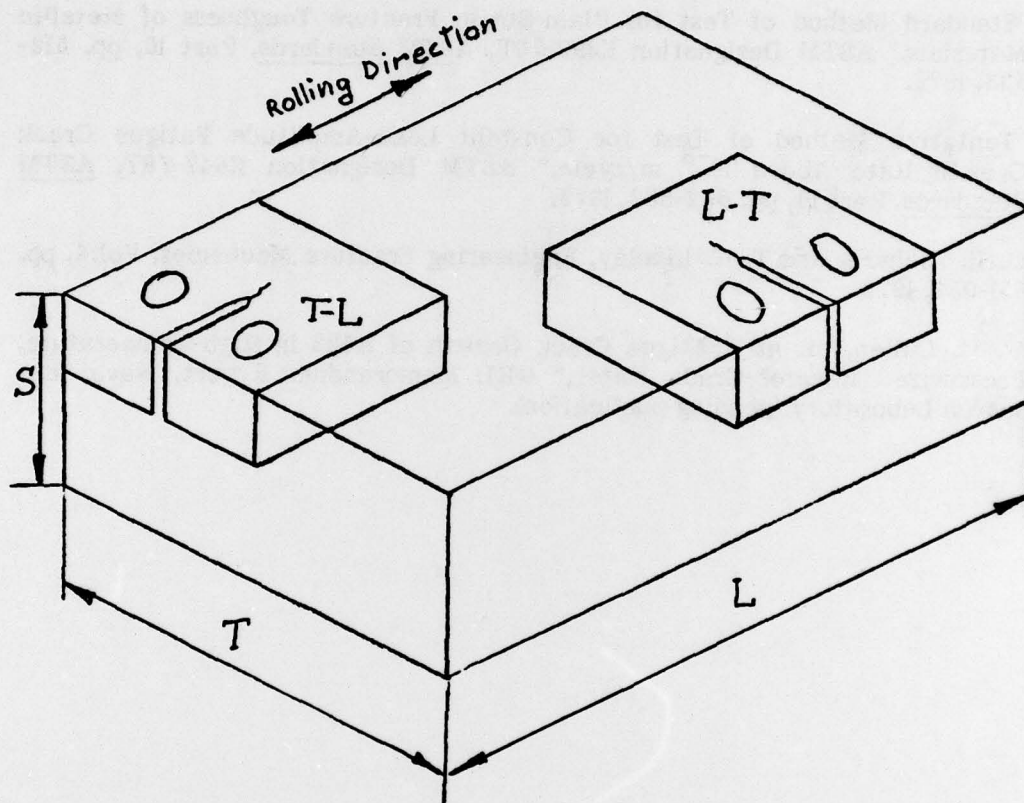


Fig. 1 Schematic diagram of fatigue specimen used for mechanical tests showing L and T directions.

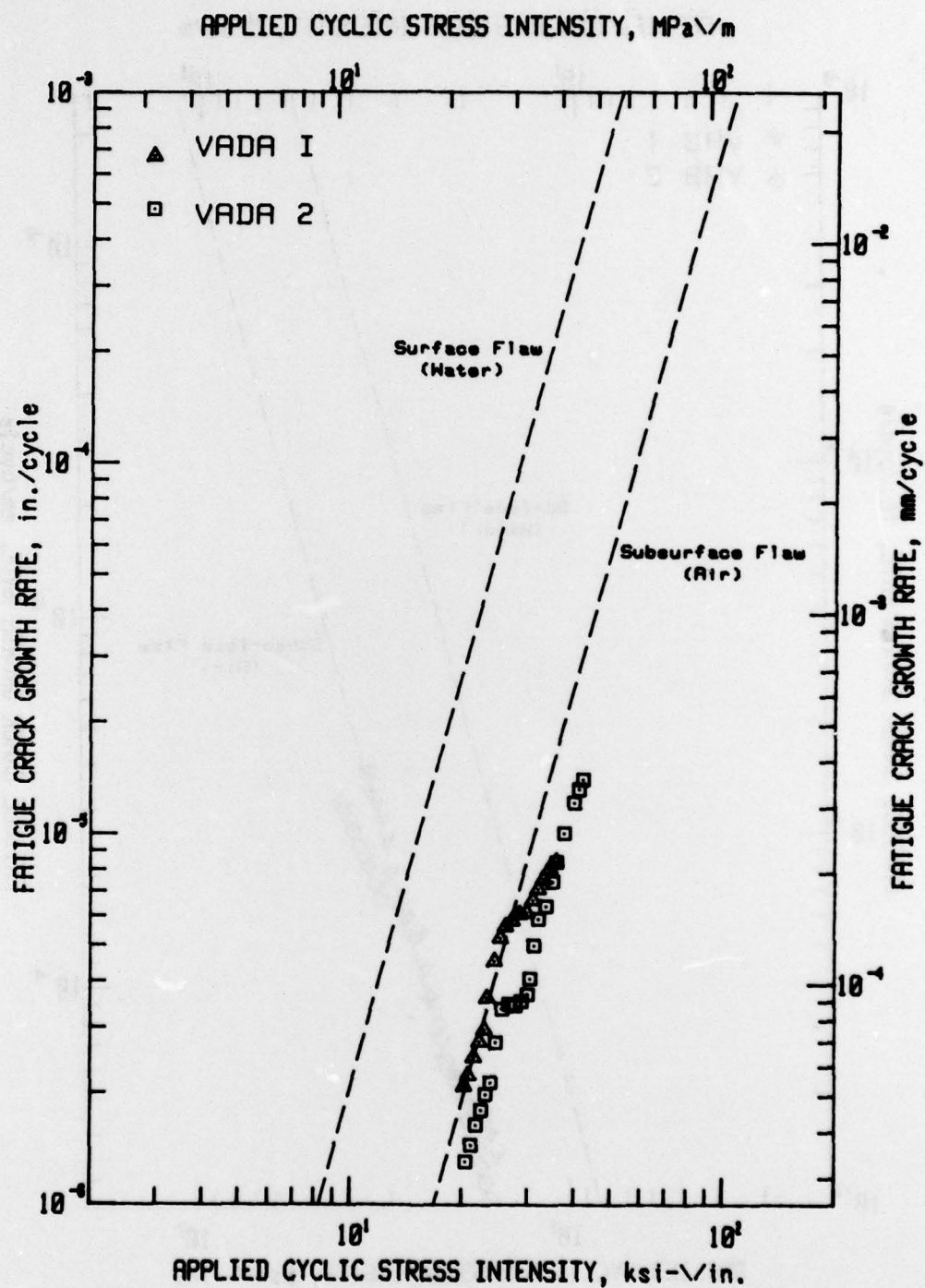


Fig. 2 Fatigue crack propagation data of A302-B ferritic steel tested in air at room temperature both for the T-L (VADA1) and L-T (VADA2) directions with the higher starting  $\Delta K$  value ( $22 \text{ MPa}\sqrt{\text{m}}$ ).

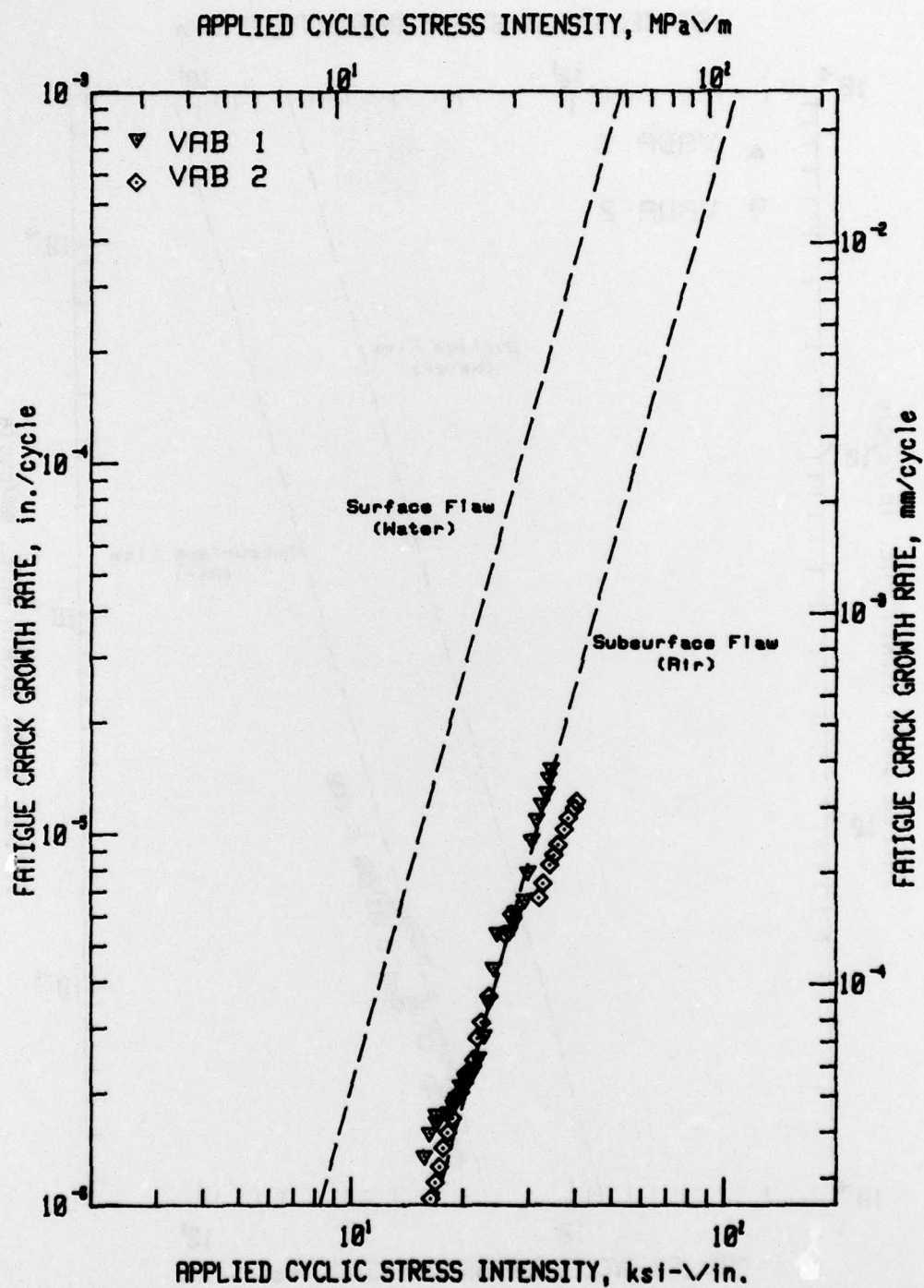


Fig. 3 Fatigue crack propagation data of A302-B ferritic steel tested in air at room temperature both for the T-L (VAB1) and L-T (VAB2) directions with the lower starting  $\Delta K$  value (16.5 MPa√m).

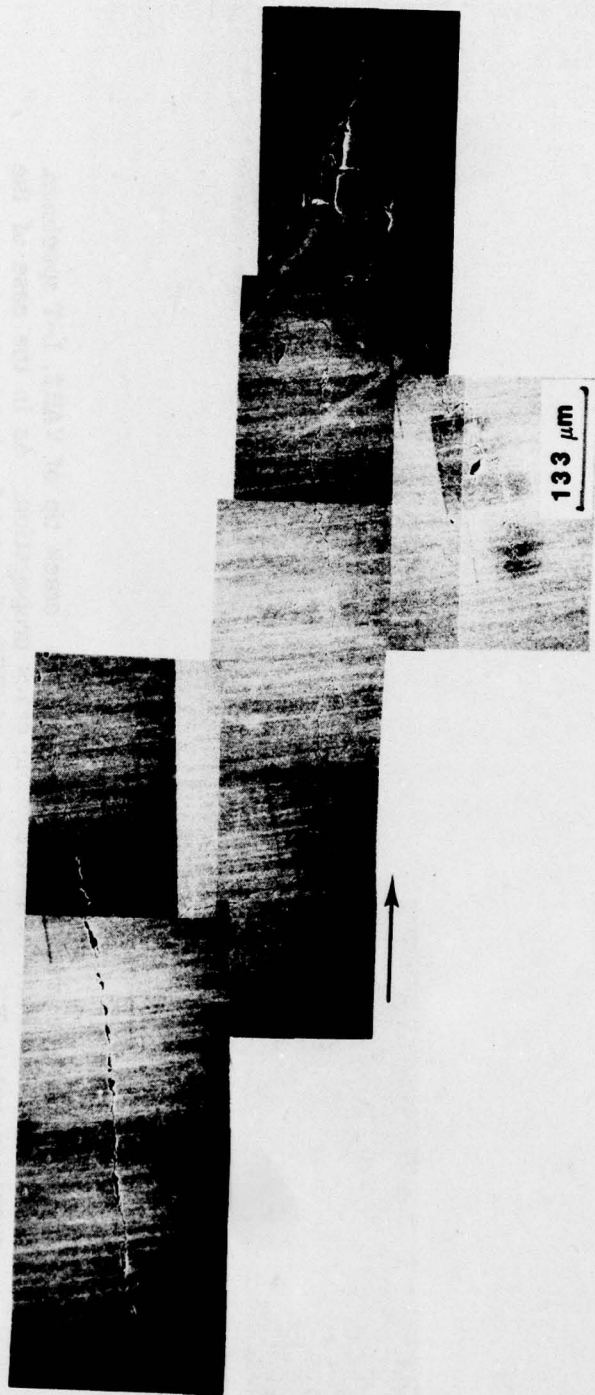


Fig. 4 Fatigue crack profile close to the crack tip of VAB1, T-L specimen. Arrow indicates direction of macroscopic crack propagation. Series of SEM micrographs show extensive microbranching near crack tip region; some branching runs perpendicular to main crack path.

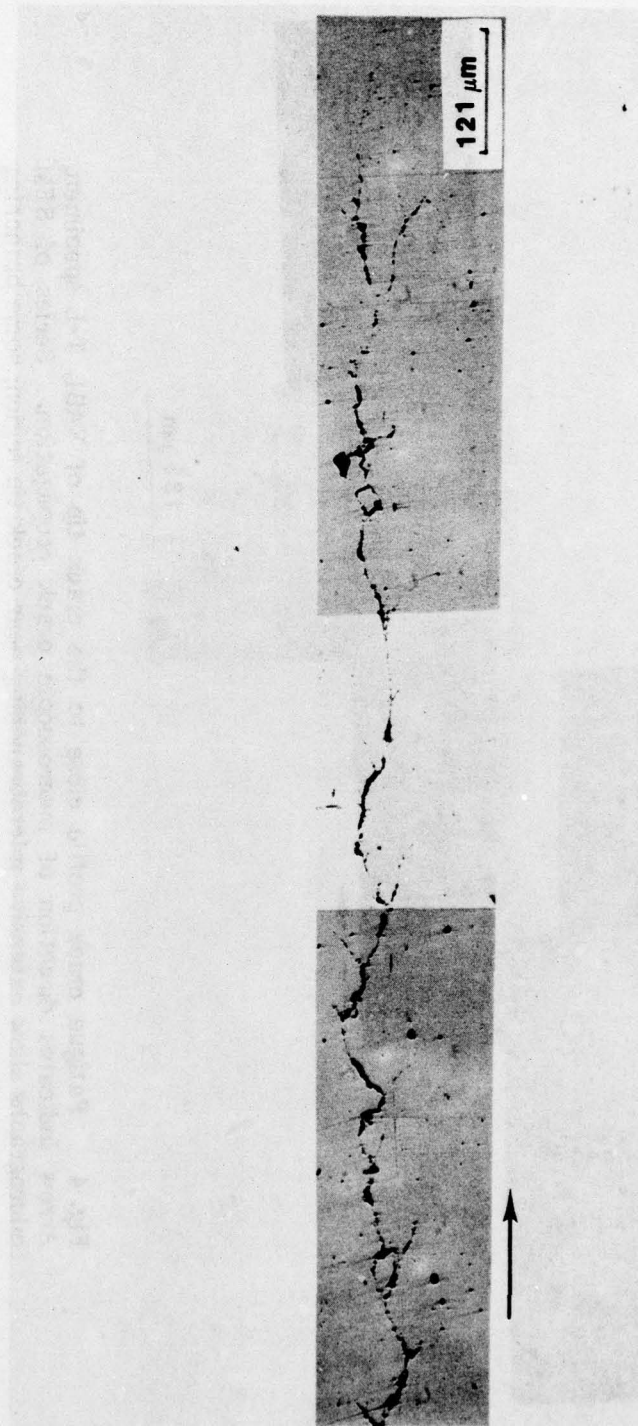


Fig 5 Fatigue crack profile close to the crack tip of VAB2, L-T specimen. Arrow show direction of macroscopic crack propagation. As in the case of the specimen cut in T-L direction, series of SEM micrographs show extensive micro-branching along the main crack path.



Fig. 6 Fracture surface of A302-B ferritic steel specimen cut along T-L direction (VADAl) tested in air at room temperature with higher starting  $\Delta K$  value. Arrow shows direction of macroscopic crack propagation. SEM micrographs clearly show inclusion bands in the fracture surface that run parallel to the macroscopic crack propagation direction.



**Fig. 7** Fracture surface of A302-B ferritic steel specimen cut along T-L direction (VAB1), tested in air at room temperature with the lower starting  $\Delta K$  value. Arrow shows direction of macroscopic crack propagation. Series of SEM micrographs show transition region corresponding to 25-30 MPa $\sqrt{m}$   $\Delta K$  value, where inclusion bands begin to appear in fracture surface.



Fig. 8 Fracture surface of A302-B ferritic steel specimen cut along the L-T direction (VADA2), tested in air at room temperature with higher starting K value. Arrow shows direction of macroscopic crack propagation. SEM micrographs illustrate transgranular failure mode with fatigue striations and extensive secondary cracking perpendicular to main crack path. These fractographic features are typical of ferritic steels tested under analogous conditions.

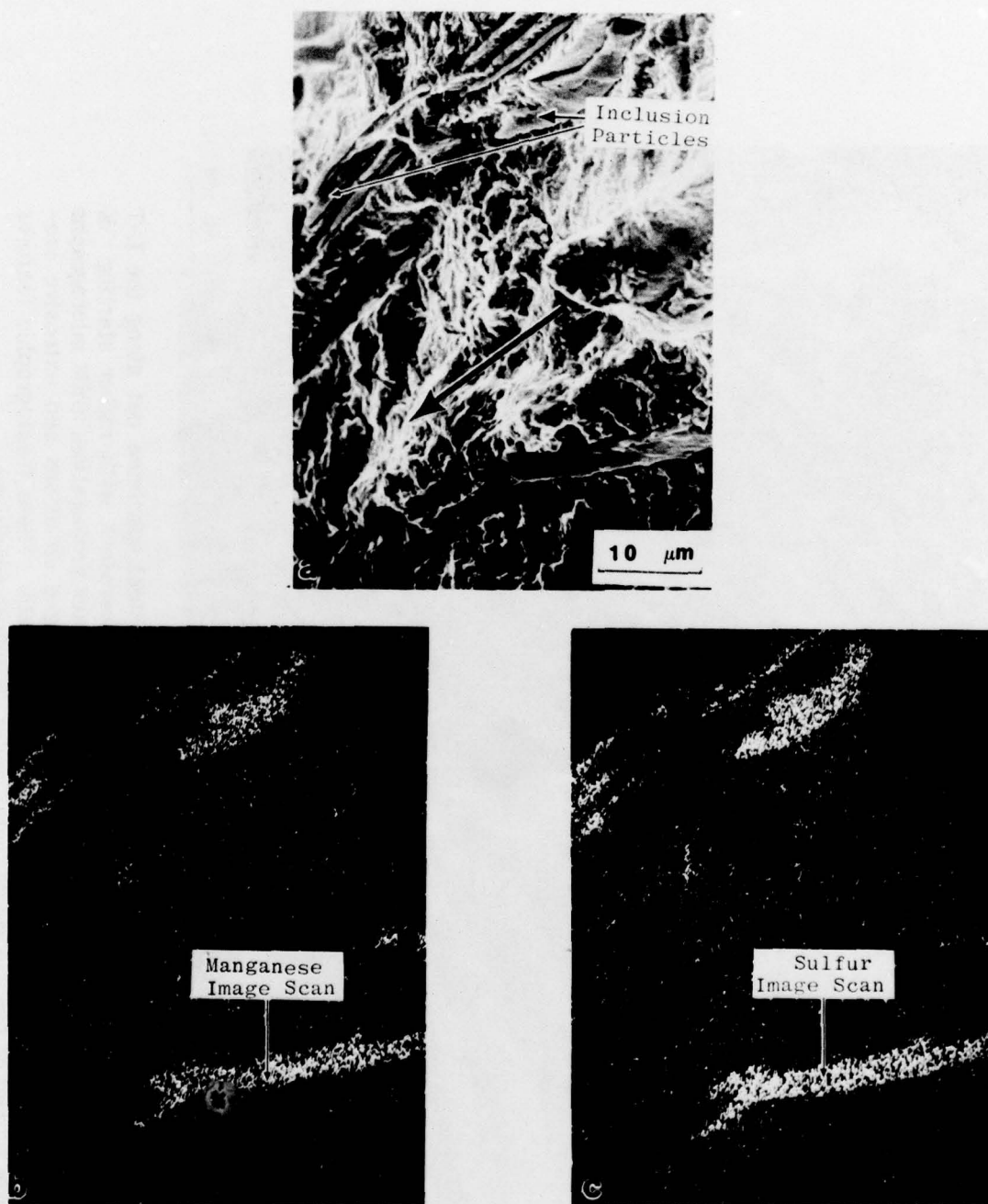


**Fig. 9** Fracture surface and corresponding energy dispersive X-ray point maps of A302-B ferritic steel specimen cut along T-L direction (VAB1). Arrow shows macroscopic crack propagation direction. SEM micrograph on top of the figure (micrograph a) clearly shows inclusion bands in the fracture surface that run parallel to the macroscopic crack propagation direction. Lower two micrographs are image scans obtained through energy dispersive X-ray microanalysis showing that inclusion bands are manganese (left) and sulfur (right) second-phase particles.

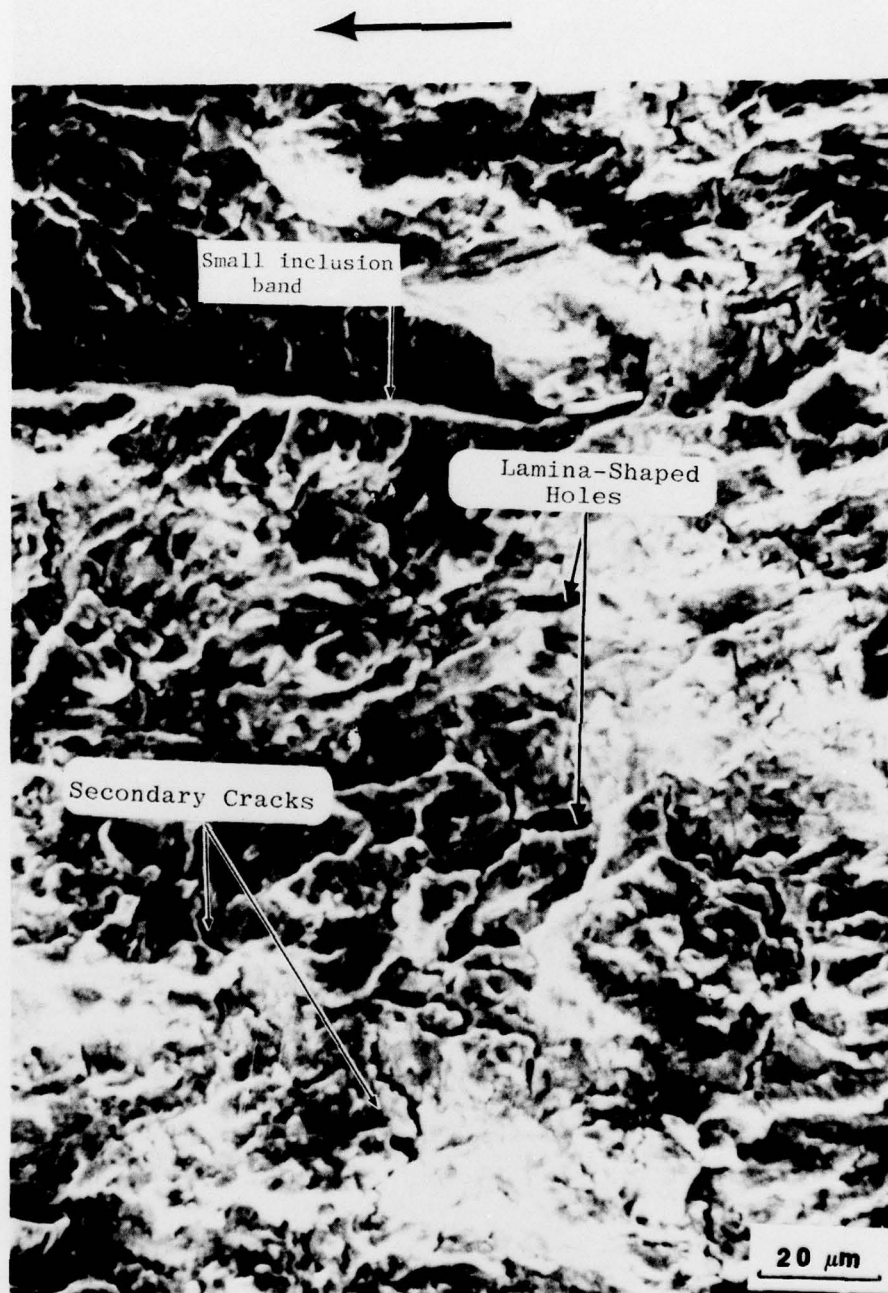


Fig. 10 Fracture surface of A302-B ferritic steel specimen cut along L-T direction (VADA2) tested in air at room temperature. Arrow shows direction of macroscopic crack propagation. SEM micrograph shows small inclusions and lamina-shaped holes present in the fracture surface. The lamina-shaped holes are believed to represent the inclusion bands that are oriented perpendicular to main crack plane.